Eur. Phys. J. C 8, 457–463 (1999)
DOI 10.1007/s100529901081

THE EUROPEAN PHYSICAL JOURNAL C

Radiative effects in processes of diffractive vector meson electroproduction

I. Akushevich

National Center of Particle and High Energy Physics, Bogdanovich str. 153, 220040 Minsk, Belarus (e-mail: aku@hep.by)

Received: 23 August 1998 / Published online: 15 April 1999

Abstract. The electromagnetic radiative correction to the cross section of the vector meson electroproduction is calculated. Explicit covariant formulae for the observed cross section are obtained. The dependence of the radiative correction on the experimental resolution and on the inelasticity cut is discussed. The FORTRAN code DIFFRAD, based on both exact (ultrarelativistic) and approximate sets of the formulae for the radiative correction to the cross section, is presented. Detailed numerical analysis for kinematical conditions of the recent experiments on the diffractive electroproduction of vector mesons is given.

1 Introduction

The measurement of the cross section of the exclusive vector meson electroproduction can provide information on the hadronic component of the photon and on the nature of diffraction. Over several years, the diffractive production of the vector meson has been the subject of muon production [1–3] and electroproduction [4–6] experiments. Data analysis of these experiments is affected considerably by QED radiative effects. In practice, the radiative corrections (RC) to the processes of electroproduction are taken into account by using codes originally developed for the inclusive case (see [7], for example).

The purpose of this paper is to calculate the electromagnetic correction to experimentally observed cross sections for the kinematics of fixed target and collider experiments directly. The Feynman diagrams necessary to calculate RC are presented on Fig. 1.

In order to calculate exactly the QED RC to the cross section of vector meson production, the method offered in [8] is used. By exact formulae we mean the expressions for the lowest-order RC obtained without any approximations but ultrarelativistically: the lepton mass m is considered to be small. In Sect. 2 the kinematics of the radiative and non-radiative processes and exact formulae for the lowest-order RC are obtained. In Sect. 3 the analytical results are visualized by the construction of the approximate formulae for cases interesting in practice. The numerical results are given in Sect. 4. A brief discussion and conclusions are given in Sect. 5.

2 Exact formulae for the lowest-order correction

Seven kinematical variables are necessary to describe the radiative process of diffractive vector meson production

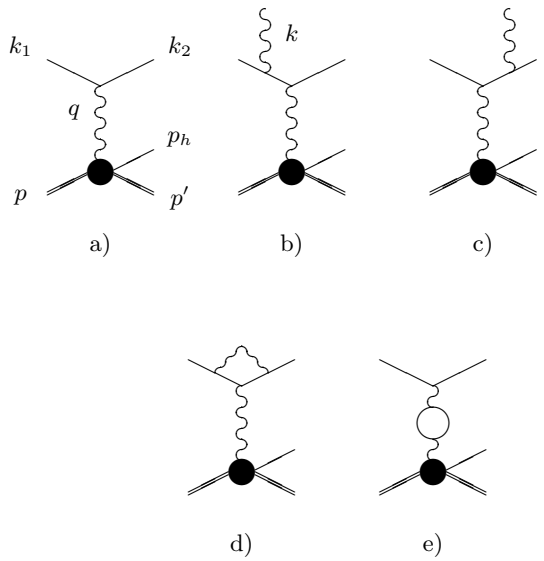

Fig. 1. Feynman diagrams contributing to the Born and the next-order cross sections. The letters denote the four-momenta of corresponding particles

(Fig. 1b,c). Four of them are the same as for the non-radiative case: the usual scaling variables x and y, the negative square of momentum transferred from the virtual photon to the proton $t = (q - p_h)^2$ and the angle ϕ_h between the scattering $(\mathbf{k_1}, \mathbf{k_2})$ and production $(\mathbf{q}, \mathbf{p_h})$ planes in the laboratory frame. The squared virtual photon momentum $Q^2 = -(k_1 - k_2)^2$ and the invariant mass of the initial proton and the virtual photon $W^2 = (p+q)^2$ are often used instead of x and y. The kinematics of a real photon is described by three additional variables [9,

10]: the inelasticity $v = \Lambda^2 - M^2$ (M is the proton mass and $\Lambda^2 = (p' + k)^2$ is the squared invariant mass of the system of unobserved particles), $\tau = kq/kp$ and the angle ϕ_k between planes $(\mathbf{k_1}, \mathbf{k_2})$ and $(\mathbf{q}, \mathbf{k})$.

We consider the RC to three- and four-dimensional cross sections $\sigma = \mathrm{d}^4\sigma/\mathrm{d}x\mathrm{d}y\,\mathrm{d}t\mathrm{d}\phi_h$ and $\bar{\sigma} = \mathrm{d}^3\sigma/\mathrm{d}x\mathrm{d}y\mathrm{d}t$. They are related as

$$\bar{\sigma} = \int_0^{2\pi} \mathrm{d}\phi_h\, \sigma\ . \tag{1}$$

The four differential Born cross section can be presented in the form

$$\sigma_0 = \frac{\alpha}{4\pi^2 xy}\left(y^2\sigma_T + 2\big(1 - y - \frac{1}{4}y^2\gamma^2\big)(\sigma_L + \sigma_T)\right), \tag{2}$$

where σ_T and σ_L are differential cross sections of the photoproduction, $\gamma^2 = Q^2/\nu^2$ and ν is the virtual photon energy.

The differential cross section of the radiative process has the following form:

$$\sigma_\mathrm{R} \propto \frac{|M_\mathrm{b} + M_\mathrm{c}|^2}{4\ k_1 p}\mathrm{d}v\frac{\mathrm{d}^3k}{2k_0}\delta\left((\Lambda - k)^2 - M^2\right), \tag{3}$$

where $\Lambda = p + q - p_h$ and $M_{b,c}$ are matrix elements of the processes given in Fig. 1b,c. In order to extract the infrared divergence and form it into a separate term we follow [8] and use the identity

$$\sigma_\mathrm{R} = \sigma_\mathrm{R} - \sigma_\mathrm{IR} + \sigma_\mathrm{IR} = \sigma_\mathrm{F} + \sigma_\mathrm{IR}, \tag{4}$$

where σ_F is finite for $k \to 0$ and σ_IR is the infrared divergent part

$$\sigma_\mathrm{IR} = \frac{\alpha}{\pi}\delta_\mathrm{R}^\mathrm{IR}\sigma_0 = \frac{\alpha}{\pi}(\delta_\mathrm{S} + \delta_\mathrm{H})\sigma_0. \tag{5}$$

The quantities δ_S and δ_H appear after splitting the integration region over v by the infinitesimal parameter $\bar{v}$:

$$\delta_\mathrm{S} = \frac{1}{\pi}\int_0^{\bar{v}} \mathrm{d}v \int \frac{d^{n-1}k}{(2\pi\mu)^{n-4}k_0}F_\mathrm{IR}\delta\left((\Lambda - k)^2 - M^2\right),$$

$$\delta_\mathrm{H} = \frac{1}{\pi}\int_{\bar{v}}^{v_\mathrm{m}} \mathrm{d}v \int \frac{\mathrm{d}^3k}{k_0}F_\mathrm{IR}\delta\left((\Lambda - k)^2 - M^2\right), \tag{6}$$

where μ is an arbitrary parameter of the mass dimension, v_m is a maximal inelasticity and

$$F_\mathrm{IR} = \frac{m^2}{(2kk_1)^2} + \frac{m^2}{(2kk_2)^2} - \frac{Q^2 + 2m^2}{(2kk_1)(2kk_2)}. \tag{7}$$

The way to calculate integrals like (6) has been offered in [8] (see also the review [11]). In our case we have

$$\delta_\mathrm{S} = 2\left(P_\mathrm{IR} + \log\frac{\bar{v}}{\mu M}\right)(l_\mathrm{m} - 1) + \log\frac{S'X'}{m^2M^2} + S_\phi,$$

$$\delta_\mathrm{H} = 2(l_\mathrm{m} - 1)\log\frac{v_\mathrm{m}}{\bar{v}}, \tag{8}$$

where $l_\mathrm{m} = \log(Q^2/m^2)$. The quantities $S' = 2\Lambda k_1 = S - Q^2 - V_1$ and $X' = 2\Lambda k_2 = X + Q^2 - V_2$ are calculated by using $V_{1,2} = 2(a_{1,2} + b\cos\phi_h)$, where

$$a_1 = \frac{1}{2\lambda_q}(Q^2S_pS_t - (SS_x + 2M^2Q^2)t_q),$$

$$a_2 = \frac{1}{2\lambda_q}(Q^2S_pS_t - (XS_x - 2M^2Q^2)t_q),$$

$$b = \frac{1}{\lambda_q}(Q^2S_t^2 - S_tS_xt_q - M^2t_q^2 - m_v^2\lambda_q)^{1/2} \times (SXQ^2 - M^2Q^4 - m^2\lambda_q)^{1/2}. \tag{9}$$

The invariants are defined as

$$S = 2k_1p,\ X = 2k_2p = (1 - y)S,\ Q^2 = Sxy,$$
$$S_{p,x} = S \pm X,\ S_t = S_x + t,\ t_q = t + Q^2 - m_v^2,$$
$$\lambda_q = S_x^2 + 4M^2Q^2. \tag{10}$$

The infrared terms P_IR, parameters μ and $\bar{v}$ and the squared logarithms containing the mass singularity l_m^2 are completely canceled in the sum of $\delta_\mathrm{R}^\mathrm{IR}$, with δ_V coming from a contribution of the vertex function (Fig. 1d):

$$\delta_\mathrm{V} = -2\left(P_\mathrm{IR} + \log\frac{m}{\mu}\right)(l_\mathrm{m} - 1) - \frac{1}{2}l_\mathrm{m}^2 + \frac{3}{2}l_\mathrm{m} - 2 + \frac{\pi^2}{6}. \tag{11}$$

For this sum we have

$$\frac{\alpha}{\pi}(\delta_\mathrm{S} + \delta_\mathrm{H} + \delta_\mathrm{V}) = \delta_\mathrm{inf} + \delta_\mathrm{VR}, \tag{12}$$

where

$$\delta_\mathrm{VR} = \frac{\alpha}{\pi}\left(\frac{3}{2}l_\mathrm{m} - 2 - \frac{1}{2}\log^2\frac{X'}{S'} + \mathrm{Li}_2\left(1 - \frac{Q^2M^2}{S'X'}\right) - \frac{\pi^2}{6}\right),$$

$$\delta_\mathrm{inf} = \frac{\alpha}{\pi}(l_\mathrm{m} - 1)\log\frac{v_\mathrm{m}^2}{S'X'}. \tag{13}$$

Here we used the ultrarelativistic expression for S_ϕ calculated in [12]. The higher-order corrections can be partially taken into account by using a special procedure of exponentiation of the multiple soft photon radiation. There is an uncertainty: what part of δ_VR has to be exponentiated? Within the considered approach [12] $(1 + \delta_\mathrm{inf})$ is replaced by $\exp\delta_\mathrm{inf}$.

For the observed cross section of the vector meson electroproduction we obtain

$$\sigma_\mathrm{obs} = \sigma_0\mathrm{e}^{\delta_\mathrm{inf}}(1 + \delta_\mathrm{VR} + \delta_\mathrm{vac}) + \sigma_\mathrm{F}. \tag{14}$$

The correction δ_vac comes from the effects of vacuum polarization by leptons and hadrons (Fig. 1e). The explicit QED formulae for the first one can be found in [9]. The hadronic contribution is given by a fit coming from the data on $\mathrm{e}^+\mathrm{e}^- \to$ hadrons [13].

The contribution of the infrared finite part can be written in terms of POLRAD 2.0 notation [9,10]:

$$\sigma_{\rm F} = -\frac{\alpha^2 y}{16\pi^3}\int\limits_0^{2\pi}{\rm d}\phi_k \int\limits_{\tau_{\min}}^{\tau_{\max}}{\rm d}\tau \sum_{i=1}^{2}\sum_{j=1}^{3}\theta_{ij} \times \int\limits_0^{v_m}\frac{{\rm d}v}{f}R^{j-2}\left(\frac{\mathcal{F}_i}{\tilde{Q}^4}-\delta_j\frac{\mathcal{F}_i^0}{Q^4}\right), \quad (15)$$

where $R=v/f$, $f=1+\tau-\mu$ and $2M\tau_{\rm max,min}=S_x\pm\sqrt{\lambda_q}$; $\delta_j=1$ for $j=1$ and $\delta_j=0$ otherwise.

The quantities θ_{ij} depend on only the kinematical invariants and the integration variables τ and ϕ_k :

$$\begin{aligned}
\theta_{11} &= 4Q^2F^0_{\rm IR},\\
\theta_{12} &= 4\tau F^0_{\rm IR},\\
\theta_{13} &= -2(2F+F_d\tau^2),\\
\theta_{21} &= 4(SX-M^2Q^2)F^0_{\rm IR},\\
\theta_{22} &= -F_dS_p^2\tau+F_{1+}S_pS_x+2F_{2-}S_p\\
&\quad -4F^0_{\rm IR}M^2\tau+2F^0_{\rm IR}S_x,\\
\theta_{23} &= 4FM^2+2F_dM^2\tau^2-F_dS_x\tau-F_{1+}S_p,
\end{aligned} \quad (16)$$

where

$$F_d=\frac{F}{z_1z_2}, F_{1+}=\frac{F}{z_1}+\frac{F}{z_2}, F_{2\pm}=F\left(\frac{m^2}{z_2^2}\pm\frac{m^2}{z_1^2}\right), \quad (17)$$

$F=1/(2\pi\sqrt{\lambda_Q})$ and $F^0_{\rm IR}=F_{2+}-Q^2F_d=F_{\rm IR}R^2$. The quantities $\mu=kp_h/kp=2(a_k+b_k\cos(\phi_h-\phi_k))$ and $z_{1,2}=kk_{1,2}/kp=2(a^z_{1,2}-b^z\cos\phi_k)$ include the dependence on angles:

$$\begin{aligned}
a_1^z &= \frac{1}{2\lambda_q}(Q^2S_p+\tau(SS_x+2M^2Q^2)),\\
a_2^z &= \frac{1}{2\lambda_q}(Q^2S_p+\tau(XS_x-2M^2Q^2)),\\
a_k &= \frac{1}{2\lambda_q}((2Q^2+\tau S_x)S_{\rm m}-(S_x-2\tau M^2)t_q),\\
b^z &= \frac{1}{\lambda_q}(SXQ^2-M^2Q^4-m^2\lambda_q)^{1/2}\\
&\quad\times(Q^2+\tau S_x-\tau^2M^2)^{1/2},\\
b_k &= \frac{1}{\lambda_q}(Q^2S_{\rm m}^2-S_{\rm m}S_xt_q-M^2t_q^2-m_v^2\lambda_q)^{1/2}\\
&\quad\times(Q^2+\tau S_x-\tau^2M^2)^{1/2}.
\end{aligned} \quad (18)$$

Here $S_{\rm m}=S_t-v$.

The dependence on the photoproduction cross sections is included in $\mathcal{F}_i$:

$$\begin{aligned}
\mathcal{F}_1 &= (S_x-R)\sigma_{\rm T}^R, \quad \mathcal{F}_2=\frac{2\tilde{Q}^2}{S_x-R}(\sigma_{\rm T}^R+\sigma_{\rm L}^R),\\
\mathcal{F}_1^0 &= S_x\sigma_{\rm T}, \qquad\qquad \mathcal{F}_2=2x(\sigma_{\rm T}+\sigma_{\rm L}).
\end{aligned} \quad (19)$$

The quantities $\sigma_{\rm T,L}$ have to be calculated for Born kinematics, but $\sigma^R_{\rm T,L}$ is calculated in terms of so-called true kinematics. It means that they have to be calculated for the tilde variables

$$\begin{aligned}
\tilde{Q}^2 &= Q^2+R\tau,\\
\tilde{W}^2 &= W^2-R(1+\tau),\\
\tilde{t} &= t+R(\tau-\mu)
\end{aligned} \quad (20)$$

instead of the usual Q^2, W^2 and t.

The important point is the dependence of the results on the maximal inelasticity $v_{\rm m}$. The inelasticity is calculated in terms of the measured momenta, so it is possible to make a cut on the maximal value of this quantity. If this cut is not applied the maximal inelasticity is defined by kinematics only. Below, we give the formulae for $v_{\rm m}$ in terms of the kinematical invariants,

$$4Q^2v_{\rm m}=\left(\sqrt{\lambda_q}-\sqrt{t_q^2+4m_v^2Q^2}\right)^2 -(S_x-2Q^2+t_q)^2-4M^2Q^2, \quad (21)$$

and in terms of kinematical limits on t,

$$v_{\rm m}=\frac{1}{C}(t_{\max}-t)(t-t_{\min}), \quad (22)$$

where C behaves for small t as

$$C=\frac{Q^2+m_v^2}{2W^2}\left(S_x+\sqrt{\lambda_q}\right)+O(t). \quad (23)$$

The maximal inelasticity given by kinematics is plotted in Fig. 2 in the kinematical points close to experiments on fixed targets. For collider experiments the shape of $v_{\rm m}$ is similar. The position of the peak and its maximum value are calculated as

$$\begin{aligned}
t_{\rm peak} &= -\frac{m_v}{W}(S_x-2Q^2),\\
v_{\rm m}(t_{\rm peak}) &= (W-m_v)^2-M^2.
\end{aligned} \quad (24)$$

3 The approximation

The structure of the exact formulae for the cross section of the hard bremsstrahlung $\sigma_{\rm F}$ obtained in the last section is not simple. Here we analyze them under approximation. The third integration variable v is not a completely photonic one. It is calculated from the measured momenta of the final lepton and the vector meson. For non-radiated events $v\equiv 0$. In practice, however, the distribution over v has a Gaussian form due to the finite resolution. Radiative effects also affect the distribution (see Sect. 4.3). So a cut on the invariant mass of the unobserved system rejects events with hard radiated photons and helps to reduce the total RC. Below, we consider the approximation based on the assumption that $v_{\rm m}$ is relatively small or a kinematical cut on v is used. Also, for diffractive scattering the squared momentum t transferred to the hadronic system is always small, so we construct the approximate

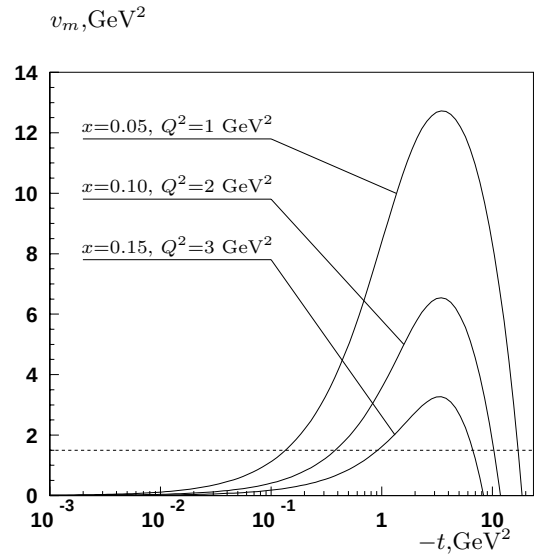

Fig. 2. Maximal inelasticity for $\rho(770)$ electroproduction. The dashed line gives a possible cut

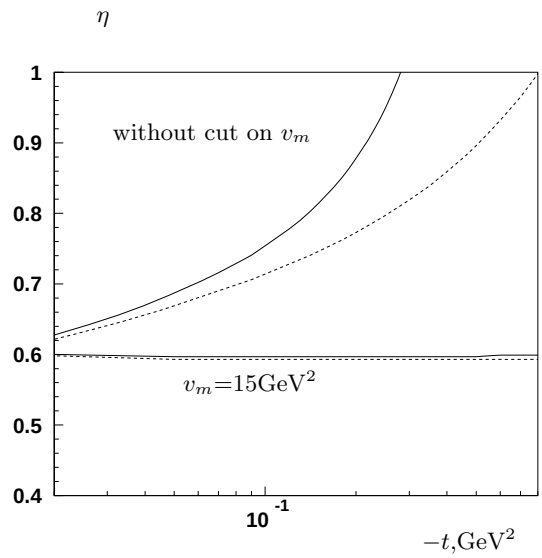

Fig. 3. RC factor (29) for $\rho(770)$ electroproduction calculated with exact (solid line) and approximate (dashed line) formulae within the kinematical conditions of the HERA collider experiment; $\sqrt{S} = 300$ GeV, $Q^2 = 3$ GeV^2, $W^2 = 5000$ GeV^2.

formulae for RC to the cross section $\mathrm{d}^3\sigma/\mathrm{d}x\mathrm{d}y\mathrm{d}t$ with an additional assumption

$$M^2 \ll S,\ t \ll Q^2. \tag{25}$$

It is clear that this condition is normal for the collider experiments but it is often not so bad for fixed target experiments as well. Due to the smallness of v_m we can keep only leading terms in the expansion of the integrand (15) over v. The first non-vanishing term contains the first derivative of the integrand. The main contribution to this derivative comes from the factor $\exp(b_v t)$ (b_v is a slope parameter), which describes the slope of the observed cross section with respect to $-t$ in most models of $\sigma_{\mathrm{L,T}}$. It is not difficult to keep all the contributions to the derivative but for simplicity we restrict our calculation to this contribution. In this case

$$\frac{1}{v}\left(\frac{Q^4}{\tilde{Q}^4}\frac{\mathcal{F}_i}{\mathcal{F}_i^0} - 1\right) \approx b_v \frac{\tau-\mu}{1+\tau-\mu} \tag{26}$$

and it is possible to integrate over ϕ_h, ϕ_k and τ explicitly:

$$\frac{1}{2\pi}\int\limits_0^{2\pi} \mathrm{d}\phi_h \frac{\tau-\mu}{1+\tau-\mu} \approx \frac{Q^2+m_v^2}{S_x - Q^2 - m_v^2},$$
$$\int\limits_0^{2\pi} \mathrm{d}\phi_k \int\limits_{\tau_{\min}}^{\tau_{\max}} \mathrm{d}\tau F_{\mathrm{IR}}^0 = -2\,(l_\mathrm{m}-1)\,. \tag{27}$$

The final result for $\bar{\sigma}_\mathrm{F}$ (see (1)) is simply

$$\bar{\sigma}_\mathrm{F} = \frac{2\alpha b_v v_\mathrm{m}}{\pi}(l_\mathrm{m}-1)\frac{Q^2+m_v^2}{S_x - Q^2 - m_v^2}\bar{\sigma}_0. \tag{28}$$

Apart from a simple analytical form, the formula obtained has one more advantage. The correction depends on only the kinematical variables, not on the dynamical characteristics of the interaction, σ_T and σ_L. It allows a possible systematical error coming from the choice of the model to be eliminated. Such systematics could be large because we have to know the differential cross sections σ_T and σ_L in the varying wide region of four variables, but there are neither enough experimental data for that nor satisfactory models. Using (28) we have systematics coming from the approximate formulae instead of exact ones. But we are able to control it by comparing the values calculated from (15) and (28) by using any model.

Moreover there is the possibility to provide the 'event by event' procedure, reweighting each event with the RC factor. The comparison of the results for the cross sections with and without this reweighting gives the correction.

Figure 3 demonstrates the accuracy of the constructed approximation with and without using the cut on inelasticity. For small values of $-t$ the exact and approximate results are in agreement for both cases; however, in the case of large $-t$ ($-t \sim 0.1\mathrm{GeV}^2$) the approximation can be used only along with the cut.

4 Numerical analysis and the code DIFFRAD

In this section we present the FORTRAN code DIFFRAD, which was created on the basis of the exact formulae in Sect. 2. The program calculates the lowest-order RC to the diffractive vector meson electroproduction. The higher-order effects are approximated by the procedure of exponentiation. The formulae for the cross section are given in a covariant form, so the code can be run both for the fixed target experiments and for the experiments at the

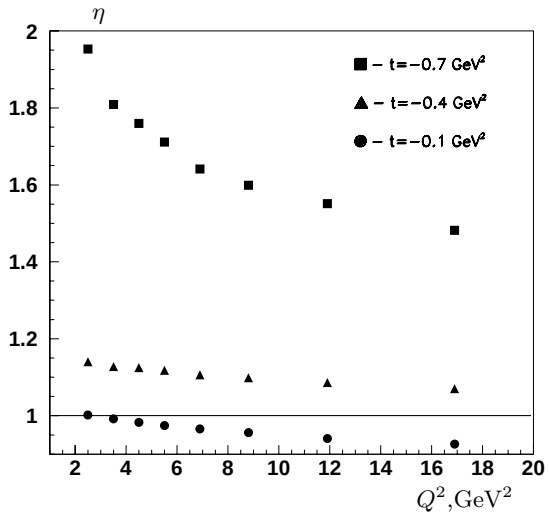

Fig. 4. RC factor for $\rho(770)$ muon production under the kinematical conditions of EMC/NMC; $\sqrt{S} = 19.4$ GeV; $\langle W^2 \rangle = 210$ GeV^2. No cut on inelasticity is used

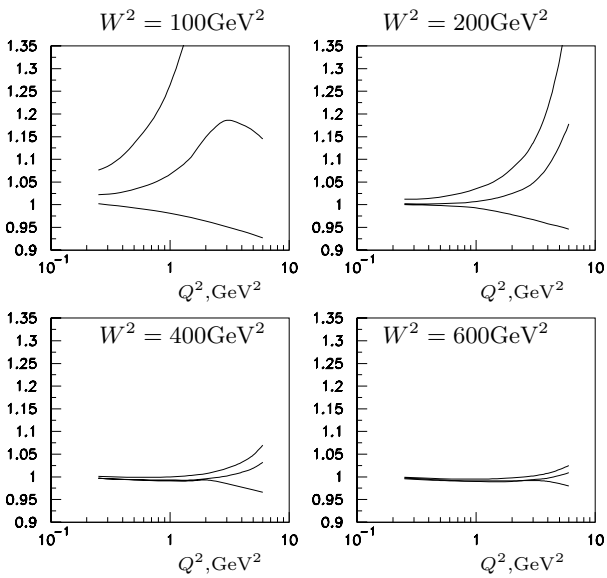

Fig. 5. RC factor for $\rho(770)$ muonproduction under the kinematical conditions of E665 using a cut on maximal inelasticity $v_{\rm m} = 15$ GeV^2. $\sqrt{S} = 30$ GeV. Curves from top to bottom correspond to $t = -0.9$, -0.5, -0.1 GeV^2

collider. The model for $\sigma_{\rm L,T}$ presented originally in [14] and developed in [15] is used as an input.

Below we give numerical results for the RC factor

$$\eta = \frac{\bar{\sigma}_{\rm obs}}{\bar{\sigma}_0} = \frac{\int\limits_0^{2\pi} {\rm d}\phi_h \sigma_{\rm obs}}{\int\limits_0^{2\pi} {\rm d}\phi_h \sigma_0} \qquad (29)$$

and t and v distributions obtained within the kinematical regions of recent experiments on the leptoproduction of vector mesons.

4.1 RC to the cross section

In Fig. 4 one can see Q^2 and t dependences of the RC factor η in the kinematical region of the EMC and NMC experiments. There is no cut on inelasticity used. For high values of t the RC can reach a factor of two. The reason for such a large effect is the smallness of the Born photoproduction cross sections $\sigma_{\rm L,T}$. They fall as $\exp(b_v t)$. In the observed cross section this factor is in the integral and there is a contribution from the region on t where $\sigma_{\rm L,T}$ are not so small. As a result $\sigma_{\rm obs}$ falls with the increasing $-t$ but not so fast.

Figure 5 gives the results for η within the kinematics of the experiment E665 with a cut on the inelasticity. Note that it can be done because of the rather good resolution over v (standard deviation σ of its distribution is smaller than the $v_{\rm m}$ given by kinematics). Use of this cut leads to different behavior of η as a function of Q^2. The different plots on this figure give the W^2 dependence of η.

The dependence of η on the kinematical variables Q^2 and t in the region of the collider experiments at HERA is presented in Fig. 6. No cut on inelasticity is used, so the

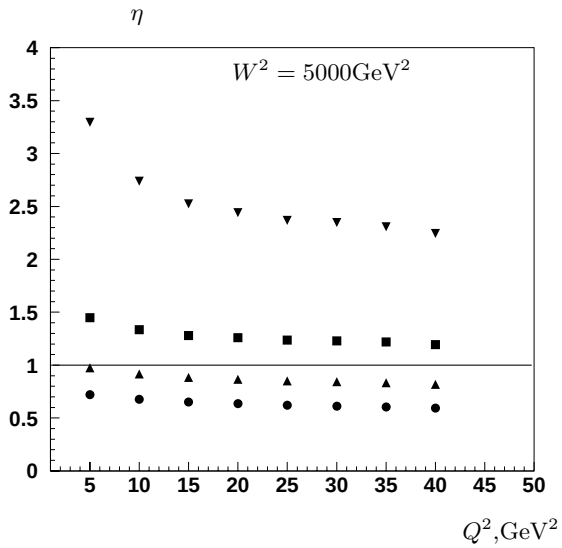

Fig. 6. RC factor for ρ (770) electroproduction under hte kinematical conditions of collider experiments at HERA; $\sqrt{S} = 300$ GeV. Symbols from top to bottom correspond to $t = -0.7$, -0.5, -0.3, -0.1 GeV^2. No cut on inelasticity is used

Q^2 dependence is similar to one given for the EMC/NMC experiment. It is found that the RC factor η is not sensitive to W^2. This is due to the fact that the photoproduction cross section is almost flat in the kinematical region of the collider experiments.

The dependence on the $v_{\rm m}$ cut in the region of HERMES kinematics is analyzed in Fig. 7. Use of the cut changes the RC factor for small Q^2 and does not influence it for larger values of Q^2, which can be seen in Fig. 2. In the case of cut usage we have to define $v_{\rm m}$ as the minimum value of the cut and the $v_{\rm m}$ given by the kinematical

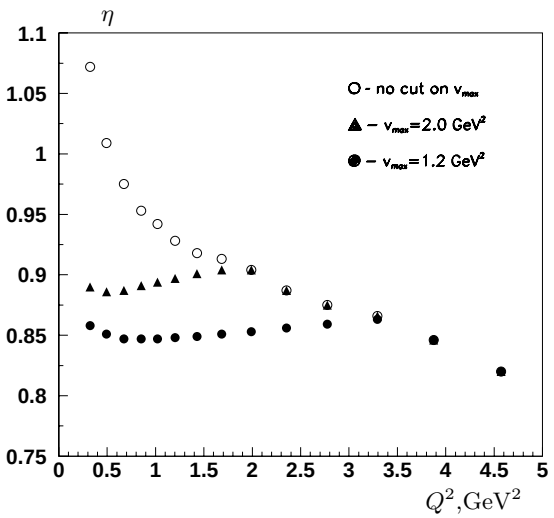

Fig. 7. RC factor $\rho(770)$ electroproduction under the kinematical conditions of HERMES. $\sqrt{S} = 7.9$ GeV, $t = -0.11$ GeV^2, $\langle y \rangle = 0.55$

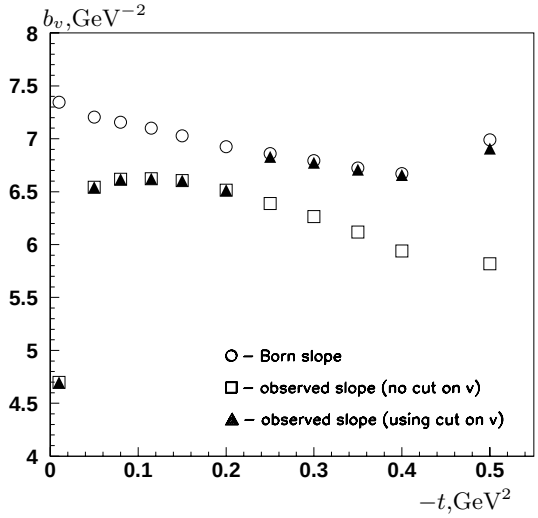

Fig. 9. Slope parameter for $\rho(770)$ muonproduction with respect to $-t$. $\sqrt{S} = 30$ GeV, $Q^2 = 2$ GeV^2, $W^2 = 200$ GeV^2. $v_m = 15$ GeV^2

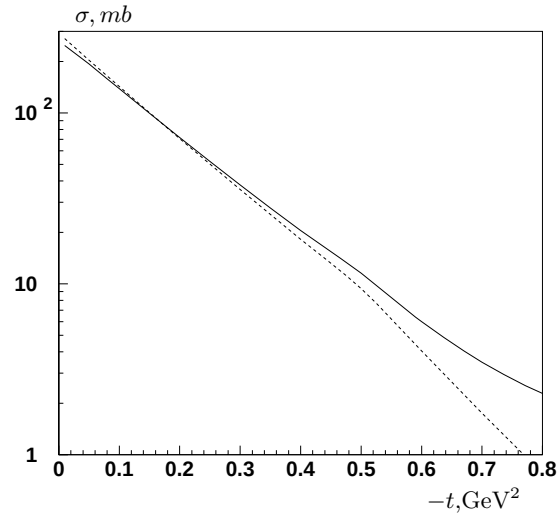

Fig. 8. The Born (dashed) and observed (solid) cross sections of $\rho(770)$ muonproduction with respect to $-t$. $\sqrt{S} = 30$ GeV, $Q^2 = 2$ GeV^2, $W^2 = 200$ GeV^2. No cut on inelasticity is used

restrictions (21). For fixed values of $-t$ the cut influences $v_{\rm m}$ and RC up to certain value of Q^2 only.

4.2 t distribution

The radiative effects can influence the slope of the observed cross section with respect to $-t$ because of the dependence of RC on this variable. It is illustrated in Figs. 8 and 9. The Born and observed slopes are calculated as a first derivative over t of the logarithm of the Born and observed cross sections. The t dependence of the Born cross section within the model of [14,15] is basically defined by a two-gluon form factor taken in exponential form, $\exp(b_v t)$ with $b_v = 5$ GeV^{-2}. We note that the slope of the Born cross section is about 6.5–7.5 GeV^{-2} in Fig. 9 and is not equal to b_v exactly. This is due to the dependence on the transverse momentum of the vector meson $p_t^2 \approx -t$ (see (2-4) in [15]).

Taking RC into account leads to a reduction in the slope of the observed cross section of the order of 10%. An additional dependence on t in the case of RC comes basically from $v_{\rm m}$, which is proportional to $t - t_{\rm min}$ in the diffractive region of small $-t$. Owing to this fact, both the exponent $\exp(\delta_{inf})$ and the cross section $\sigma_{\rm F}$ tend to zero when $t \to t_{\rm min}$. So the observed cross section vanishes in this limit.

4.3 Inelasticity distribution

In this section we discuss influence of RC on the inelasticity distribution. There are several reasons for the inelasticity to be non-zero: the finite experimental resolution, radiative effects and the mixture of non-exclusive inelastic events. The last of these is usually suppressed by experimental methods, and we neglect it here.

Inelasticity v is calculated in terms of the momenta of the final lepton and vector mesons, which are experimentally measured. The Born cross section does not depend on inelasticity, so the inelasticity distribution is a pure Gaussian with a mean value equal to zero and a standard deviation σ defined by the experimental resolution. However, since there is v dependence in the RC (see the integrand of (15)) the observed inelasticity distribution deviates from simple Gaussian form. To see the difference we generate the Born and observed inelasticity distributions (see Fig. 10). The first one is generated as a pure Gaussian (solid line). The following procedure is applied for the generation of the observed distribution. First, the

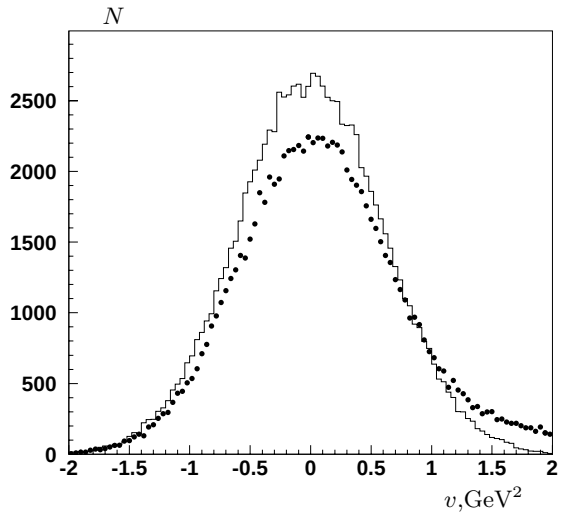

Fig. 10. Inelasticity distributions for $\rho(770)$ electroproduction: Born (line) and radiatively corrected (circles); $\sqrt{S} = 7.9$ GeV, $x = 0.01$, $y = 0.75$, $-t = 0.15$ GeV^2, $\sigma = 0.7$ GeV^2, $v_m = 2$GeV^2

type of process being radiated or non-radiated is generated in accordance with their contributions to the total observed cross section. The non-radiated events include Born processes, loop effects and the radiation of soft photons, whose energy does not exceed one standard deviation σ of the Born distribution. They do not change the kinematics of the Born process, so their inelasticity distribution is generated in accordance with the Gaussian distribution as well. Inelasticity of radiated events is generated in according to $\mathrm{d}\sigma_f/\mathrm{d}v$ in the region $\sigma < v < v_\mathrm{m}$ with smearing of each generated v over the Gaussian distribution with a standard deviation equaling σ. The observed distribution is presented on Fig. 10 (closed circles).

5 Discussion and conclusion

In this article, the QED radiative effects have been analyzed in kinematics of recent experiments on the exclusive vector meson electroproduction. The explicit covariant formulae for RC to the cross section are given in (13–15). An approximate expression for the bremsstrahlung cross section can be found in (28).

The RC to the cross section of the diffractive vector meson electroproduction is very sensitive to the cut on the inelasticity. Using a harder cut leads to smaller values of the RC factor.

In the diffractive region ($-t < 0.3$) RC is negative and can reach

- 10% for muon experiments with fixed target,
- 20% for electron experiments with fixed target,
- 40% for electron collider experiments.

This large effect comes basically from a double logarithmic contribution in δ_inf (13). For example, for collider kinematics both its logarithms exceed 10, and δ_inf can reach 0.5.

There is no essential dependence on the type of vector meson. All the numerical results are given for the case of ρ meson production. The dependence on the type of scattered lepton is typical. RC in the case of the electron scattering is several times larger due to the appearance of the lepton mass in the argument of the leading logarithm.

The Born cross section has a steeper slope with respect to t than the observed cross section does. The RC to the slope parameter is negative and about 10%.

The FORTRAN code DIFFRAD is available (aku@hep.by) for the calculation of the RC to observable quantities in experiments on the diffractive vector meson electroproduction.

Acknowledgements. I am grateful to A. Brull and N. Shumeiko for help and support. Also I would like to thank N. Akopov, A. Borissov, A. Droutskoi, E. Kuraev, P. Kuzhir, A. Nagaitsev, M. Ryskin, A. Soroko and H. Spiesberger for fruitful discussions and comments.

References

1. EMC Collaboration, J.J. Aubert et al., Phys. Lett. B **161**, (1985) 203
2. NMC Collaboration, M. Arneodo et al., Nucl. Phys. B **429**, (1994) 503
3. E665 Collaboration, M.R. Adams et al., Z. Phys. C **74**, 237 (1997)
4. H1 Collaboration; S. Aid et al., Nucl. Phys. B **468**, (1996) 3
5. ZEUS Collaboration; M.Derrick et al., Phys. Lett. B **356**, (1995) 601
6. HERMES Collaboration; M.Tytgat for the collaboration, Vector Meson Production at HERMES, Proceedings of the DIS98 Workshop, Brussels, Belgium, April 1998, World Scientific. (to be published)
7. K.Kurek, DESY 96-209, 1996, hep-ph/9606240
8. D.Yu.Bardin, N.M.Shumeiko, Nucl. Phys. B **127**, (1977) 242
9. I.V.Akushevich, N.M.Shumeiko, J. Phys. G **20**, (1994) 513
10. I.Akushevich, A.Ilyichev, N.Shumeiko, A.Soroko, A.Tolkachev, Comp. Phys. Comm. **104**, (1997) 201
11. A.Akhundov, D.Bardin, L.Kalinovskaya, T.Riemann, Fortsch. Phys. **44**, (1996) 373
12. N.M.Shumeiko, Sov. J. Nucl. Phys. **29**, (1979) 807
13. H.Burkhardt, B.Pietrzyk, Phys.Lett. B **356**, (1995) 398
14. M.G. Ryskin, Z.Phys. C **57**, (1993) 89
15. M. Arneodo, L. Lamberti, M. Ryskin, Comp. Phys. Comm. **100**, (1997) 195